

# Airborne Radiometric Data: A Tool for Reconnaissance Geological Mapping Using a GIS\*

## Abstract

Airborne gamma ray spectrometer data collected by the Geological Survey of Canada, gridded to a pixel resolution of 125 metres, is used to create digital images that show the spatial distributions of gamma ray spectrometer (radiometric) data: equivalent Uranium (eU), equivalent Thorium (eTh), and Potassium (%K). These radioelement images are currently used by the Geological Survey to assist in geological mapping and mineral exploration. Data interpretation is traditionally made visually from hardcopy of pseudo-colored single-channel images, or from three-channel color composite images. Visual interpretation can be augmented by using an unsupervised classification procedure on the radioelement data. The resulting clusters are displayed as an image, and interpreted by digitally overlaying the digitized geological map. This brings out the similarities and differences between units determined from field mapping and units based on radioelement response.

Images of the three radioelement channels were input to a migrating-means cluster analysis on an image processing system. The resulting classified image was imported into a GIS. Other data sets in the GIS included table-digitized bedrock and surficial geology maps and a binary map showing the presence of water bodies, derived from a density sliced Landsat Thematic Mapper band 5 image. Lakes and bogs, as well as regions covered by particular surficial units, were combined into a new binary image used to mask out regions where the radioelement response was unrelated to outcrop. The classified radioelement image was then compared with the geological map using two-map overlay and area analysis cross-tabulation techniques.

The cross-tabulation clearly identifies those geological units that have a distinctive radioelement response. By reclassifying the map overlay, by imposing a color coding scheme that enhances bedrock geology classes, the relationship between the bedrock geology and radioelement response is enhanced. The degree of correlation between the two cartographic images is site dependent, rather than global, as might be expected. The correlation is not simply on the basis of the average radioelement values, but also on the shape, texture, and extent of the radioelement clusters. Areas where the two maps differ indicate zones of possible interest for

field verification of published field maps for the purposes of mineral exploration.

Despite the relatively low spatial resolution of the gamma ray spectrometer data, the areas studied show quite strong spatial associations between the radioelement clusters and bedrock units. The overlay technique was helpful in isolating inconsistencies between the two classified maps, suggesting sites for further localized field mapping.

## Objectives

The purpose of the present study is to apply a clustering technique to radioelement data and to compare the resulting cluster map with a digitized geological map within a GIS software package. This procedure should lead to a better understanding of the relationship between geological map units and radioelement patterns and help to identify locations where more detailed field work is needed. This work will serve to demonstrate the utility of image analysis and GIS within the Geological Survey of Canada.

## Background

Migrating-means clustering has been found to be an effective technique for grouping pixels with similar radioelement signatures into classes. Harris (1989) showed that radioelement clusters were strongly correlated with mapped geology in the Meguma Terrane of eastern Nova Scotia.

Three-channel color composite plots prepared by the Geological Survey of Canada (GSC, 1990) and Intensity, Hue, and Saturation (IHS) color composites prepared by the Canada Centre for Remote Sensing (Graham and Ford, 1991; Harris *et al.*, 1990) reveal striking relationships and also apparent discrepancies with geological mapping at a regional scale. The three-channel image is created by the display of eU as red, eTh as green, and K as blue to create a color composite. For the Geological Survey enhancement (GSC, 1990), specific lookup tables are used for each channel for an optimum product with the color strength modulated by total count.

In the case of the IHS transform enhancements (Graham and Ford, 1991), the radioelement images are assigned to red, green, and blue channels, followed by a transformation to the IHS coordinate system. The resulting Hue reflects variations in all three radioelements. The Intensity information is replaced by Canada Centre for Remote Sensing airborne radar data and the Saturation variable is held constant at a maximum 8-bit value of 255. In the reverse transform of the IHS back to RGB color space, the radar data are effectively merged

\*Presented at the Ninth Thematic Conference on Geologic Remote Sensing, Pasadena, California, 8-11 February 1993.

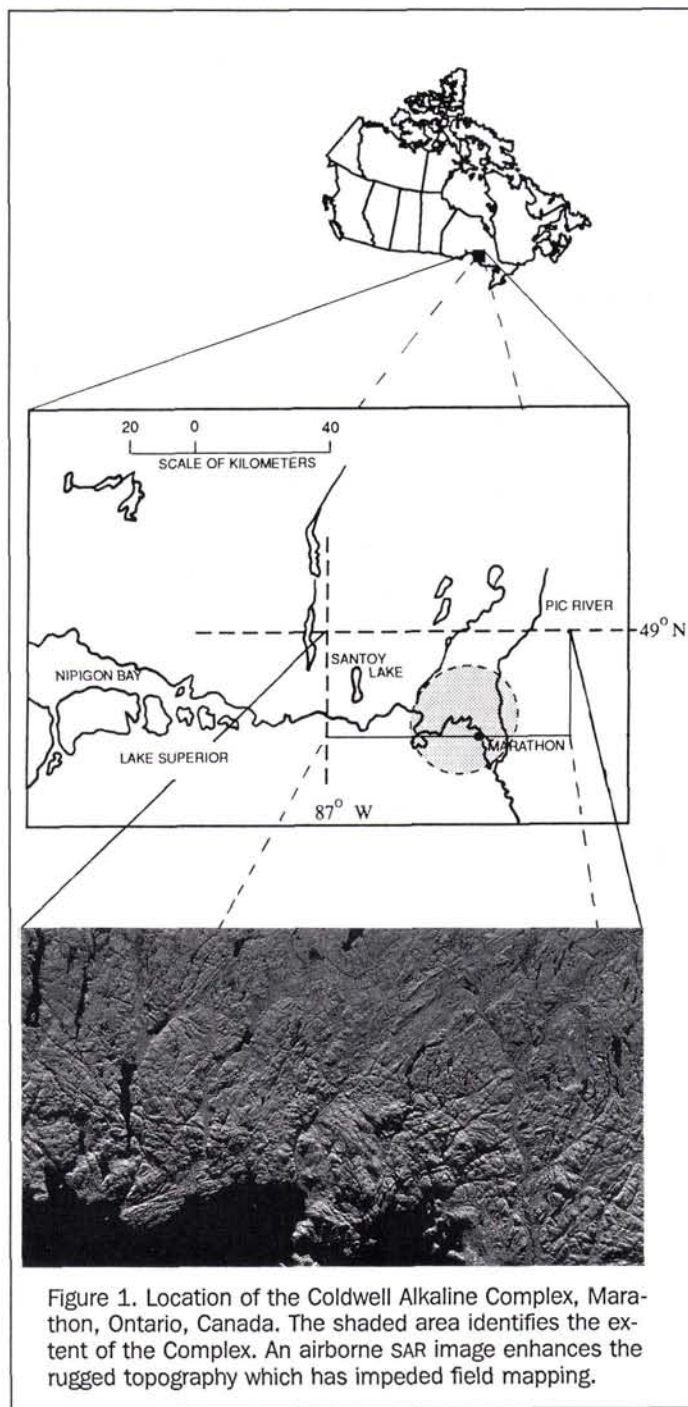


Figure 1. Location of the Coldwell Alkaline Complex, Marathon, Ontario, Canada. The shaded area identifies the extent of the Complex. An airborne SAR image enhances the rugged topography which has impeded field mapping.

with the radiometric data. Radiometric data are a measure of the concentration of radioelements, providing information on surface cover and in some cases lithology. Radar, because of its side viewing geometry, enhances terrain morphology and surface roughness. Radar data, in the IHS transform, provide a good high resolution cartographic base for the presentation of radiometric data, which is useful for reconnaissance mapping.

### Location and Geology

Marathon is situated along the north shore of Lake Superior between the towns of Schreiber in the west and Hemlo in the

east. The study area is on 1:50,000-scale NTS map sheets 42D/9, 15, and 16. A Canada Centre for Remote Sensing airborne radar image enhances the area's rugged topography which, along with dense vegetation, has greatly impeded field mapping (Figure 1).

The general area hosts several precious metal (Hemlo - Au) and base metal (Winston Lake - Zn, Cu, Ag, and Au) deposits and occurrences associated with supracrustal metavolcanic/metasedimentary sequences of the Abitibi-Wawa Subprovince of the Superior Province. In addition, numerous mineral occurrences (Ce, Nb, Cu, Fe, Ti) are hosted by the highly radioactive Coldwell Alkaline Complex, the largest alkaline intrusion in North America (Walker *et al.*, 1991).

The area is underlain by generally east-west trending metavolcanic/metasedimentary rocks occurring in supracrustal sequences of the Abitibi-Wawa Subprovince which are surrounded by poorly subdivided granitic/syenitic and gneissic lithologies. The supracrustal sequences have undergone up to four periods of deformation with large scale faulting occurring in several zones. This sequence is intruded by the Coldwell Alkaline Complex (ODM, 1972a; 1972b; Mitchell *et al.*, 1982; Schnieders and Smyk, 1989; Walker *et al.*, 1991). In general, each lithologic unit can be distinguished based on its gross radiometric signature: the Coldwell Complex is highly radioactive, the metavolcanic and sedimentary units have low to moderate radioactivity, and the granitic/gneissic units are moderate to highly radioactive. The Coldwell Complex has been interpreted as being subdivided into three centers of intrusion. To the east, ferroaugite syenite was intruded into a border gabbro. West of the first intrusion, nepheline syenite was emplaced. Between these two intrusives, a third intrusive center occurs, composed of a quartz-amphibole syenite.

### Methodology

Table 1 and Figure 2 summarize the input data used and image analysis and GIS manipulation steps. The final goal is to produce a confusion matrix showing the degree of overlap between radioelement clusters and bedrock units.

TABLE 1. SUMMARY TABLE OF DATA SOURCES.

Map/Imagery	Original Data/Legend	Digitized Classes
Bedrock Geology†	Metasediments,	1) Volcanics
	Metavolcanics, igneous rocks	
	Granite, Quartz Monzonite, Granodiorite	2) Granite
	Nepheline Syenite, Granite-Quartz Syenite	3) Quartz Syenite
	Augite Syenite	4) Augite Syenite
Surficial Geology‡	Quartz-Amphibole Syenite, Syenodiorite Hornblende, Syenite	5) Syenodiorite
	Bedrock plateaus, plains, ridges and knobs	1) Outcrop
Landsat Thematic Mapper Data	Other (Drift types)	2) Surficial Cover
	Density slice lookup table of TM band 5.	1) Water
Gamma Ray Spectrometer Data§	Migrating-means clustering of U, Th, and K.	2) Lake
		Radioelement clusters

† ODM, 1972a; 1972b.

‡ Gartner, 1980.

§ GSC, 1990.



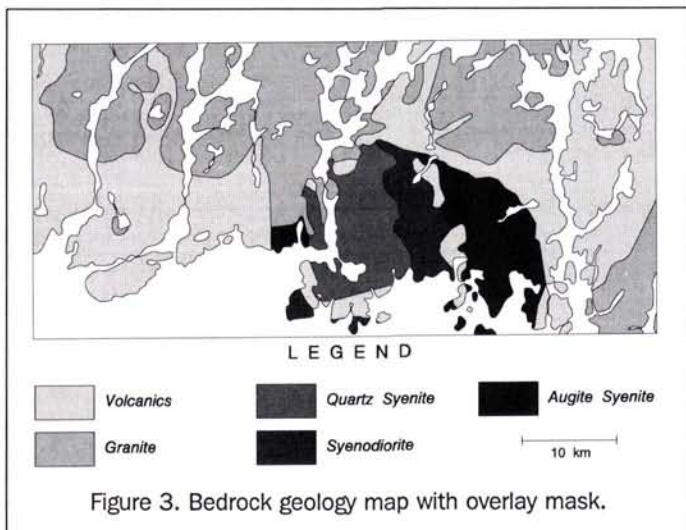


Figure 3. Bedrock geology map with overlay mask.

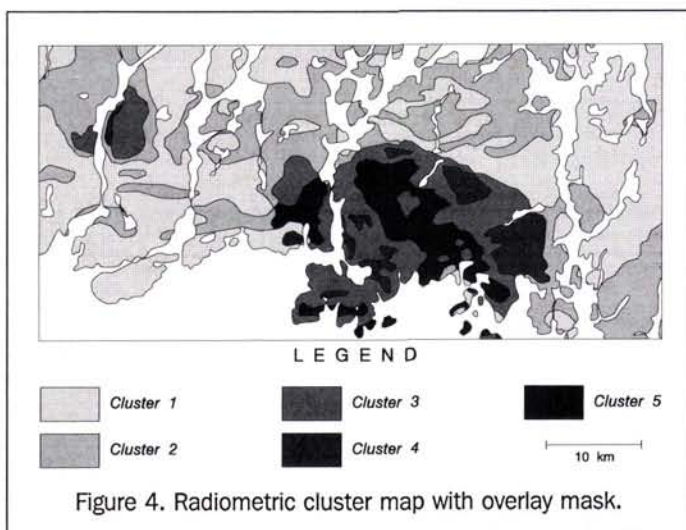


Figure 4. Radiometric cluster map with overlay mask.

mask was built by applying a threshold to the Landsat TM image (for detecting water) and the digitized map of surficial cover (Table 1). The mask was applied to both the bedrock map and the radioelement cluster map, removing the effects of water and cover from the subsequent analysis (Darnley, 1973). Figures 3 and 4 show the application of the overlay mask to the bedrock geology and radiometric cluster maps.

## Results

### Visual Evaluation

The two maps - bedrock geology (Figure 3) and radiometric clusters (Figure 4) - were combined to form an overlay map, shown in Figure 5, where each of the five cluster classes overlap each of the five bedrock classes. Based on the bedrock geology, the overlay map is coded to determine how the bedrock classes are subdivided by the radiometric cluster classes. In Figure 5, the legend annotation reflects this polygon shade pattern (i.e., **Vc1** represents the intersection of the volcanic bedrock geology class with radiometric cluster class 1. **Vc1** through **Vc5** are assigned a unique map shade pattern. The density of the shade pattern varies between cluster

classes within a single bedrock class). The resulting 25-class map shows that each radioelement class is dominantly associated with a particular bedrock unit.

The large number of classes within the Coldwell Complex indicates gradational lithologies making the separation into discrete lithologies difficult. It can be seen in Figure 4, however, that the cluster map does reveal three distinct radiometric proportions which show minor correlation with the three mapped intrusive centers found in Figure 3. Two of the Granite classes in this overlay map (Figure 5) enhance two localized targets which appear to be isolated: **A** at Santoy Lake and **B** along the northwestern edge of the Coldwell Complex, warranting further study. Confirmation of these targets by statistical means will be necessary to confirm validity.

### Analysis of Confusion Matrix

An area cross-tabulation or confusion matrix is a two-dimensional table summarizing the areal overlap of all possible combinations of the two input maps. As there are the same number of radioelement classes as there are bedrock geology map units, the confusion matrix can be arranged so that the largest elements appear in the principal diagonal. The Kappa coefficient of agreement (Rosenfeld and Fitzpatrick-Lins, 1986) then serves as a measure of correlation between the two maps.

The confusion matrix, **T** (Table 2A), is organized with the five geological map classes as columns and the radiometric clusters as the rows. Values in the matrix are areas of overlap in square kilometres. The classes are ordered within the confusion matrix such that the diagonal elements of the matrix (coincident class number) indicate the amount of agreement and the off-diagonal elements indicate the amount of disagreement or confusion. Perfectly correlated maps would have zero values in the off-diagonal positions.

To calculate the value of Kappa ( $\kappa$ ), the observed area proportions,  $p_{ij}$  (Table 2B), and the expected area proportions,  $q_{ij}$  (Table 2C), are calculated. Details relating to these computations can be found in Appendix 1.

The overall Kappa value calculated for these data is 0.46, indicating a moderately strong agreement between radiometric clusters and the generalized bedrock geology units

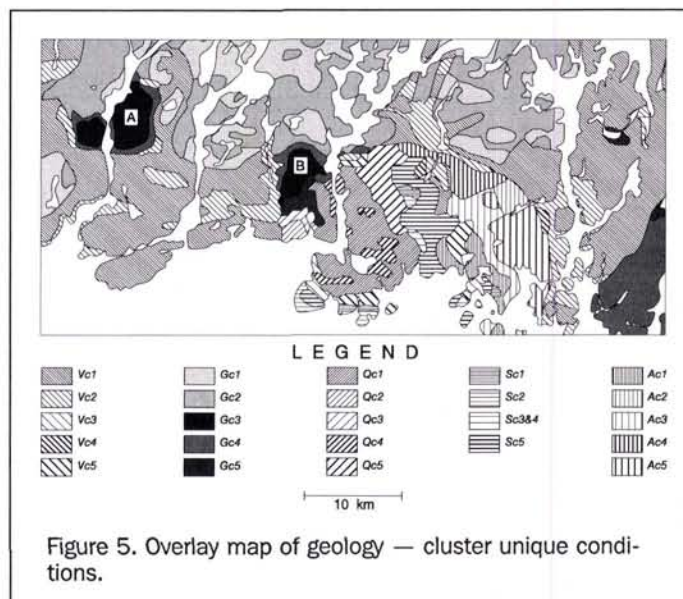


Figure 5. Overlay map of geology — cluster unique conditions.

TABLE 2. CALCULATION OF KAPPA COEFFICIENT OF AGREEMENT. (A) CONFUSION MATRIX  $T$  WITH ELEMENTS  $T_{ij}$ . (B) OBSERVED PROPORTIONS  $p_{ij}$ . SHADED VALUES IN THE PRINCIPAL DIAGONAL REPRESENT AREAS OF AGREEMENT. (C) EXPECTED PROPORTIONS  $q_{ij}$ , WITH PRINCIPAL DIAGONAL SHADED. (D) CONDITIONAL KAPPA AND PERCENT AGREEMENT.

A.		Geological Map						
Cluster Map	Class	1	2	3	4	5	Total	
	1	263.6	99.4	0.3	0.4	0.9	364.6	
2	86.7	212.9	2.9	3.8	15.9	322.2		
3	7.2	34.3	43.6	4.9	16.5	106.5		
4	10.7	9.0	24.4	27.9	11.9	83.9		
5	1.1	1.4	8.8	0.0	30.7	42.0		
Total	369.3	357.0	80.0	37.0	75.9	919.2		

B.		Geological Map						
Cluster Map	Class	1	2	3	4	5	Total	
	1	.287	.108	.0	0	.001	.396	
2	.094	.232	.003	.004	.017	.350		
3	.008	.037	.047	.005	.018	.116		
4	.012	.010	.027	.030	.013	.092		
5	.001	.002	.010	0	.033	.046		
Total	.402	.389	.087	.040	.082	1.000		

C.		Geological Map						
Cluster Map	Class	1	2	3	4	5	Total	
	1	.159	.154	.034	.016	.033	.396	
2	.140	.136	.030	.014	.030	.350		
3	.047	.045	.010	.005	.010	.117		
4	.036	.035	.008	.004	.008	.091		
5	.018	.018	.004	.002	.004	.046		
Total	.400	.388	.086	.041	.085	1.000		

D.		KAPPA	% AGREEMENT
Class	1	0.537	0.723
	2	0.445	0.661
	3	0.353	0.409
	4	0.305	0.333
	5	0.707	0.731

in exposed bedrock areas. Conditional kappa values, off-diagonal elements of the confusion matrix, and visual interpretation of the overlay map indicate several kinds of confusion. The granite (class 2) is most often confused with both the volcanics and the quartz syenite. Confusion can be expected between the volcanics and the granites because count levels are much lower than those of the Coldwell intrusive units. Of greater interest are the areas which are interpreted as quartz syenite according to the radiometric data but are mapped as granite. These visually confirmed areas of disagreement (Figure 5), again highlight targets A and B. Their spatial locations suggest areas for further detailed mapping. Target B has a strong spatial association with the Coldwell Complex, where detailed mapping may support the revision of the western limit of the intrusive body. As the radiometric classes are similar for these two targets, lithological similarities or associations may be supported by detailed field mapping.

Conditional Kappa (Table 2D) gives a value for the areal association within individual cluster classes. Cluster class 5 has greatest conditional Kappa value, indicating the best agreement occurs with the syenodiorite unit within the Coldwell Complex. In order of decreasing agreement, the volcanics are followed by the granites, quartz syenites, and augite syenite. Referring to Table 2A, the confusion matrix shows that the radiometric class 4 has almost equal area proportions associated with both the augite syenite and quartz syenite, making these two units difficult to separate radiometrically.

### Statistical Plot Evaluation

A series of box plots are used to graphically show the distribution of radiometric values within each geological class. These display the minimum, maximum, 25th percentile, 75th percentile, and mean (Figure 6). In general, the low radiometric values of the granitic and volcanic country rock distinguish them from the Coldwell Alkaline Complex units.

The unique radiometric signatures which provide the separation of colors within the initial integrated IHS images originate mainly from the contrast in the potassium results. As the K count rate is influenced by the percentage of feldspars, acidic rock types such as granite and quartz syenite show elevated values as compared to the other lithologies.

Although the box plots (Figure 6) reveal a similarity between the volcanics and granites, as compared with the syenite units, granite is distinguished by the greater potassium content. The three syenite units have relatively more eU, eTh, and K. Low eTh values of augite syenite separate it from the other syenites. The quartz syenite and syenodiorite are radiometrically quite similar, except that K is higher in the former and eU and eTh are higher in the latter.

### Conclusions

The IHS transform is a valuable algorithm for the presentation of integrated data for the purposes of reconnaissance mapping. The count rate variations of radiometric potassium predominantly control the degree of Hue separability in the IHS transform. It is proposed that the radioelement cluster

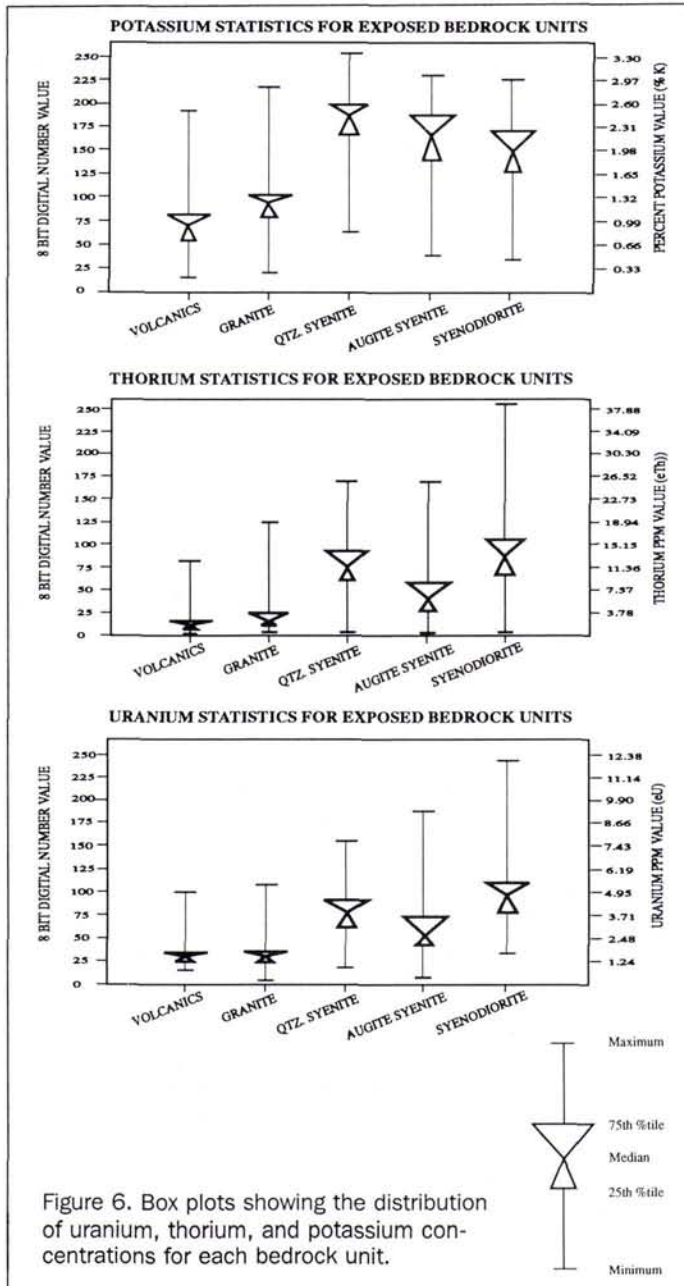


Figure 6. Box plots showing the distribution of uranium, thorium, and potassium concentrations for each bedrock unit.

mapping be considered as an additional tool for presenting gamma ray data to the geologist, in addition to the ternary IHS with radar or TM images. Cluster maps could also be combined with radar by assigning the cluster class to Hue and radar to intensity, and holding the Saturation constant.

The advantage of the clustering method is that the product is a classified image, like a geological map. The disadvantages are (1) that classifications are area-dependent and each region must be analyzed separately (i.e., clusters are not universal) and (2) that water and surficial cover need to be masked for the method to work effectively.

**Acknowledgments**

The authors would like to thank the reviewers, V. Singhroy and R. Brown of the Canada Centre for Remote Sensing

(CCRS) and J. Harris of Intera Information Technologies, for their invaluable comments. M. Trinidad of CCRS assisted in the preparation of graphics for the paper. Airborne radar data were provided by CCRS, Data Acquisition Division, while the airborne radiometric data were supplied by the Mineral Resources Division of the Geological Survey of Canada.

**References**

Darnley, A.G., 1973. Airborne Gamma Ray Survey Techniques - Present and Future, *Proceedings of a Panel on Uranium Exploration Methods*, IAEA-PL-490/15, International Atomic Energy Agency, Vienna, Austria, pp. 67-105.

Gartner, J.F., 1980. *Northern Ontario Engineering Geology Terrain Study, Data Base Map, Heron Bay*, Ontario Geological Survey, Map 5093, Scale 1:100,000.

Geological Survey of Canada (GSC), 1990. *Seven-Channel Gamma Ray Spectrometer Data Survey, Coldwell Complex, Marathon, Ontario*. Mineral Resources Division, Project leader: K.L. Ford.

Graham, D.F., and K.L. Ford, 1991. The Integration of Airborne Radar and Geophysical Data for Reconnaissance Geological Mapping in the Marathon-Schreiber Area, Northwestern Ontario, *Proceedings of the 14th Canadian Symposium on Remote Sensing*, pp. 95-98.

Harris, J.R., 1989. Clustering of Gamma Ray Spectrometer Data Using a Computer Image Analysis System, *Statistical Applications in the Earth Sciences* (F.P. Agterberg and G.F. Bonham-Carter, editors), Geological Survey of Canada, Paper 89-9.

Harris, J.R., R. Murray, and T. Hirose, 1990. IHS Transform for the Integration of Radar Imagery with other Remotely Sensed Data, *Photogrammetric Engineering & Remote Sensing*, 56(12):1631-1641.

Mitchell, R.H., and R.G. Platt, 1982. The Coldwell Alkaline Complex, Protozoic Geology of the Northern Lake Superior Area, *GAC-MAC Field Trip Guide Book*, Trip 4, Winnipeg.

Ontario Department of Mines and Northern Affairs (ODM), 1972a. *Map 2220, Manitowadge-Wawa Sheet*, Geological Compilation Series, Scale 1:253,440.

———, 1972b. *Map 2232, Nipigon-Schreiber Sheet*, Geological Compilation Series, Scale 1:253,440.

PCI, 1991. KCLUS - K-means Clustering, *EASI Pace Users Manual, Pace Multispectral Analysis Package*, V5.0a, pp 2-61 to 2-67.

Rosenfeld, G.H., and K. Fitzpatrick-Lins, 1986. A Coefficient of Agreement as a Measure of Thematic Classification Accuracy, *Photogrammetric Engineering & Remote Sensing*, 52(2):223-227.

Schnieders, B.R., and M.C. Smyk, 1989. *Annual Report for the Schreiber-Hemlo Resident Geologist's District, 1989*, Ontario Geological Survey, Miscellaneous Paper 147, pp. 139-159.

Walker, E.C., R.H. Sutcliffe, C.S.J. Shaw, and G.T. Shore, 1991. Geology of the Coldwell Alkaline Complex, *Ministry of Northern Development and Mines, Summary of Field Work and Other Activities*, Ontario Geological Survey Miscellaneous Paper 157, pp. 107-116.

**Appendix**

To calculate the kappa coefficient of agreement, an observed area proportions matrix and an expected area proportions matrix are calculated and combined using the following equations:

$$p_{ij} = \frac{T_{ij}}{T..} \tag{1}$$

where  $T..$  is the total area of comparison. Then the expected proportion,  $q_{ij}$ , is determined from

$$q_{ij} = p_i.p_j \tag{2}$$

where  $p_i$  is the marginal total for the  $i$ -th row, and  $p_j$  is the

marginal total for the  $j$ -th column of the proportions matrix. Then Kappa is

$$\kappa = \frac{\sum_{i=1}^n p_{ii} - \sum_{i=1}^n q_{ii}}{1 - \sum_{i=1}^n q_{ii}} \quad (3)$$

where  $\kappa$  ranges from  $-1$  (perfect disagreement) to  $+1$  (perfect agreement) with a value of zero indicating that the agreement is no better than that expected due to chance.

A conditional Kappa value for each cluster class can be

calculated (Figure 6d) showing the breakdown of agreement by class as shown in Equation 4: i.e.,

$$\kappa_i = \frac{p_{ii} - q_{ii}}{p_{i.} - q_{ii}} \quad (4)$$

The "percent agreement" of each cluster per geology class is simply the area proportion of a single cluster in each geology class as compared to the total area of the cluster ( $T_{ij}/T_i$ ). This measurement includes random correlations by chance which consistently over estimates the value of agreement. Kappa corrects for correlations due to chance and gives a more useful measure of areal association.

## CALL FOR PAPERS Special Issue on SOFTCOPY PHOTOGRAMMETRY

### Photogrammetric Engineering and Remote Sensing

The American Society for Photogrammetry and Remote Sensing will publish a Softcopy Photogrammetry special issue of PERS in August 1994. This issue will contain commentaries, invited and contributed articles. Authors are especially encouraged to submit manuscripts on the following topics:

- Definition issues, functional requirements, and design considerations.
- Data issues, acquisition, volume, compression, visualization, and reduction.
- Digital orthophotography, production and use.
- Softcopy photogrammetry, image analysis, and GIS, the all-in-one system concept.
- Conversion of operational production systems into softcopy, requirements and implications.
- Standards, testing procedures, accuracy, performance, and system evaluation.
- Trends in technology, state-of-the-art, and future directions.

All manuscripts, including invited articles, will be peer reviewed in accordance with established ASPRS policy for publication in PE&RS. Authors who wish to contribute papers for this special issue are invited to mail five copies of their manuscript to:

Raad A. Saleh, ERSC, University of Wisconsin-Madison, 1225 West Dayton St., Madison, WI 53706; Phone: (608) 263-6584, fax: (608) 262-5964, internet: raad@cae.wisc.edu.

- All papers should conform to the submission standards in "Instructions to Authors" that appears monthly in PE&RS.
- Papers should be free from promoting a specific commercial product.
- Papers without funds for color printing may be subject to rejection by ASPRS Headquarters due to budget constraints.
- Cover image of the special issue may be selected from one of the submitted articles. To qualify, photos must be at least 9"X9" in size, and can be prints or transparencies.
- Electronic submission will be accepted using the above e-mail address, if the manuscript contains no graphics. However, final manuscripts must be in hardcopy, accompanied by DOS ASCII disk.
- All manuscripts must be received by 5 January 1994 in order to be considered for publication in this special issue.